for sulfur dioxide + benzene and V_{int} for sulfur dioxide + cyclohexane as being entirely due to chemical interactions between sulfur dioxide and benzene. That is to say, the volume change per stoichiometric mole of sulfur dioxide [$N(SO_2)$] is given by

$$\Delta V = V_{int}(SO_2/C_6H_6) - V_{int}(SO_2/C_6H_{12}) \quad (19)$$

ΔV^θ, the standard volume change of the complexation reaction per mole of complex formed (n_{cx}), is thus

$$\Delta V^\theta = \Delta V[N(SO_2)/n_{cx}] \quad (20)$$

Combination of eq 12, 19, and 20 gives

$$\Delta V^\theta = [V_{int}(SO_2/C_6H_6) - V_{int}(SO_2/C_6H_{12})](K + 1)/K \quad (21)$$

Recommended "best" values of the molecular diameters of sulfur dioxide, benzene, and cyclohexane were taken from a critical compilation[27] and are listed in Table II. This table also lists the molar volumes and isothermal compressibilities of benzene and cyclohexane. Inserting these values into eq 14, we calculate $V_{cav}(SO_2/C_6H_6)$ and $V_{cav}(SO_2/C_6H_{12})$. Combining these values of V_{cav} with our values of $\bar{V}^\circ(SO_2/C_6H_6)$ and $\bar{V}^\circ(SO_2/C_6H_{12})$ in eq 17 leads to $V_{int}(SO_2/C_6H_6) = -60.0$ cm^3 mol^{-1} and $V_{int}(SO_2/C_6H_{12}) = -46.7$ cm^3 mol^{-1}. From eq 21 ($K = 0.47$),[3] we then calculate a value of $\Delta V^\theta = -41.6$ cm^3 mol^{-1} for the standard volume change of the benzene + sulfur dioxide complexation reaction.

Scaled particle theory might be used also to estimate ΔV^θ for other SO_2 + electron donor systems, provided that a non-electron-donating model compound with physical properties (molecular diameter, dipole moment, and polarizability) similar to those of the electron donor of interest exists.

Both of the methods we have proposed for estimating ΔV^θ for reaction 3 introduce the idea of a non-electron-donating "model" of the electron-donating solvent of interest. Our results show that ΔV^θ for the formation of the sulfur dioxide–benzene complex is large (for chemical interactions of this type) and negative. The sign of ΔV^θ indicates that the average sulfur dioxide molecule is closer to a benzene molecule than it would be in an ideal solution. This is as we would expect if sulfur dioxide and benzene are interacting chemically to form a complex.

The values of ΔV^θ for the sulfur dioxide + benzene complexation reaction obtained from the two methods differ by a factor of 2. This difference arises principally from the different way in which the contribution of uncomplexed sulfur dioxide to the total volume of the solution is taken into account. At this time, we cannot judge which of the two methods is more likely to give an accurate result.

We recommend further investigations of both the excess volumes of solutions of sulfur dioxide in benzene and the variation of the complexation equilibrium constant with pressure to provide accurate estimates of ΔV^θ. Until such information becomes available, the methods presented in this section afford reasonable estimates of the sign and magnitude of ΔV^θ.

Acknowledgment. We thank the Natural Sciences and Engineering Research Council of Canada for their support of this and related research.

(27) Mourits, F. M.; Rummens, F. H. A. *Can. J. Chem.* **1977**, *55*, 3007–3020.
(28) Tardajos, G.; Diaz-Pena, M.; Lainez, A.; Aicart, E. *J. Chem. Eng. Data* **1986**, *31*, 492–493.

Photochemistry of $(\eta^1\text{-}C_5Cl_5)Mn(CO)_5$ and $(\eta^1\text{-}C_6H_5CH_2)Mn(CO)_5$: Competitive Formation of 16- and 17e Intermediates

Kent M. Young and Mark S. Wrighton*

Contribution from the Department of Chemistry, Massachusetts Institute of Technology, Cambridge, Massachusetts 02139. *Received April 28, 1989*

Abstract: Irradiation of $RMn(CO)_5$ (R = η^1-C_5Cl_5, η^1-$C_6H_5CH_2$) in alkane glasses at 95 K leads to CO loss as the only detectable photoprocess: the ring-slipped $(\eta^3\text{-}C_5Cl_5)Mn(CO)_4$ and $(\eta^5\text{-}C_5Cl_5)Mn(CO)_3$ or $(\eta^3\text{-}C_6H_5CH_2)Mn(CO)_4$ are formed, respectively. The identities of the η^3 intermediates from $(\eta^1\text{-}C_5Cl_5)Mn(CO)_5$ and $(\eta^1\text{-}C_6H_5CH_2)Mn(CO)_5$ have been established by spectroscopic means and by chemical-trapping experiments. Room-temperature irradiation of $RMn(CO)_5$ yields both CO loss and Mn–R bond cleavage, giving $Mn(CO)_5$ and R radicals. The relative importance of these two competitive primary photoprocesses is wavelength dependent. The quantum yield for Mn–R bond homolysis is largely independent of wavelength, 436–254 nm, $\phi \cong 0.05$, whereas the CO-loss quantum yield for $(\eta^1\text{-}C_5Cl_5)Mn(CO)_5$ increases from ~0.03 at 436 nm to ~0.30 at 254 nm. The relative importance of net photoproducts is also dependent on the presence of CO, which suppresses CO-loss products. From the wavelength dependence and effects of added CO on product distribution, it is concluded that axial or equatorial CO loss from $(\eta^1\text{-}C_5Cl_5)Mn(CO)_5$ can be observed from populations of d_{z^2} or $d_{x^2-y^2}$ orbitals, respectively, with higher energy excitation favoring equatorial CO loss.

We report a quantitative study of the primary photoprocesses in $RMn(CO)_5$ (R = η^1-C_5Cl_5, η^1-$C_6H_5CH_2$). The principal aim of our work has been to establish the relative importance of CO loss and Mn–R homolysis (eq 1 and 2). In connection with CO loss (eq 1), there is also the possibility of equatorial versus axial labilization following photoexcitation.

$$RMn(CO)_5 \xrightarrow{h\nu} RMn(CO)_4 + CO \quad (1)$$

$$RMn(CO)_5 \xrightarrow{h\nu} Mn(CO)_5 + R \quad (2)$$

The photochemistry of $RMn(CO)_5$ (R = alkyl, aryl, benzyl) has been studied both in solution[1-4] and at low temperature under matrix isolation conditions.[5,6] Lappert has shown that irradiation of $RMn(CO)_5$ (R = CH_3, CH_2SiMe_3, $CH_2C_6H_5$) in solution leads to the formation of $Mn(CO)_5$ and R radicals.[2,7] Other studies

(1) (a) Geoffroy, G. L.; Wrighton, M. S. *Organometallic Photochemistry*; Academic Press: New York, 1979. (b) Pourreau, D. B.; Geoffroy, G. L. *Adv. Organomet. Chem.* **1985**, *24*, 249.
(2) Hudson, A.; Lappert, M. F.; Lednor, P. W.; Nicholson, B. K. *J. Chem. Soc., Chem. Commun.* **1974**, 966.
(3) Bamford, C. H.; Mullik, S. U. *J. Chem. Soc., Faraday Trans.* **1979**, *1*, 2562.
(4) (a) Lipps, W.; Kreiter, C. G. *J. Organomet. Chem.* **1983**, *241*, 185. (b) Kreiter, C. G.; Lipps, W. *J. Organomet. Chem.* **1983**, *253*, 339.
(5) Ogilvie, J. F. *J. Chem. Soc., Chem. Commun.* **1970**, 323.
(6) McHugh, T. M.; Rest, A. J. *J. Chem. Soc., Dalton Trans.* **1980**, 2323.

0002-7863/90/1512-157$02.50/0

have also found evidence for the production of radicals under similar conditions,[3,8] and net photoproducts, $Mn_2(CO)_{10}$, bibenzyl, and toluene from $(\eta^1\text{-}C_6H_5CH_2)Mn(CO)_5$, suggest Mn–R homolysis to be the only photoprocesses.[8] However, it has also been reported that irradiation of $RMn(CO)_5$ (R = C_6H_5, $CH_2C_6H_5$) in the presence of 1,3-dienes leads to the formation of η^3-allyl insertion products such as $Mn(CO)_4(\eta^3\text{-}C_5H_8R)$ complexes.[4] These allyl complexes presumably arise via initial CO loss followed by olefin coordination and insertion. Irradiation of $RMn(CO)_5$ (R = C_6F_5, C_2F_4H) in the presence of donor ligands has been reported to give good yields of $RMn(CO)_4L$ complexes.[9,10] The conclusion from qualitative solution photochemistry studies is that *both* CO loss and Mn–R homolysis do occur in $RMn(CO)_5$.[1-10] Under matrix isolation conditions it has been reported that $CH_3Mn(CO)_5$ loses CO upon irradiation.[5,6,11] No evidence for Mn–CH_3 bond homolysis was observed under the experimental conditions, and it was concluded that Mn–CH_3 bond homolysis is not a major primary photoprocess for this molecule in a matrix.

To explore the factors that control the reactivity of $RMn(CO)_5$ complexes that have two potential primary photoprocesses, CO loss and Mn–R bond homolysis, we have undertaken a study of the photochemistry of $(\eta^1\text{-}C_5Cl_5)Mn(CO)_5$ and $(\eta^1\text{-}C_6H_5CH_2)Mn(CO)_5$. These two molecules can form the relatively stable C_5Cl_5 or $C_6H_5CH_2$ radicals upon Mn–R bond homolysis. CO loss may lead to ring slippage, giving $(\eta^3\text{-}C_5Cl_5)Mn(CO)_4$ and $(\eta^5\text{-}C_5Cl_5)Mn(CO)_3$ or $(\eta^3\text{-}C_6H_5CH_2)Mn(CO)_4$, consistent with results already reported for $(\eta^1\text{-}C_3H_5)Mn(CO)_5$.[12]

Beyond its importance in showing the factors influencing loss of CO versus Mn–R cleavage, $(\eta^1\text{-}C_5Cl_5)Mn(CO)_5$ is also of interest because ring slippage is a possible reaction pathway following CO loss. The cyclopentadienyl ring is ubiquitous in organometallic chemistry and can have a variety of coordination geometries such as η^1, η^3, η^5, and bridging.[13] The intermediacy of slipped cyclopentadienyl rings has been proposed in many reactions of chemical significance including C–H bond activation[14] and ligand substitution.[15] However, relatively few examples of complexes containing the η^3-cyclopentadienyl ligand have been observed.[16-19] An earlier study[19] of $(\eta^5\text{-}C_5H_5)(\eta^1\text{-}C_5H_5)Fe(CO)_2$ showed that photochemical extrusion of one molecule of CO at low temperature leads to the formation of $(\eta^3\text{-}C_5H_5)(\eta^5\text{-}C_5H_5)Fe(CO)$ and eventually ferrocene thermally or upon continued photolysis at low temperature. Our new work adds additional information concerning the thermal and photochemical reactions of an η^3-cyclopentadienyl system.

Experimental Section

Instruments and Equipment. UV–vis spectra were recorded on a Cary 17 UV–vis–near-IR absorption spectrometer or on a HP 8451A diode array spectrometer. IR spectra were recorded with either a Nicolet 60SX or 170SX FTIR. ^1H and ^{13}C NMR spectra were recorded with a Varian XL300 Fourier transform spectrometer. Mass spectra were recorded on a Finnigan Mat system 8200.

IR spectra were recorded in deoxygenated alkane solutions except where noted. Solutions of the complexes were held in a cell with CaF_2 windows. Low-temperature IR spectra were recorded with the cell mounted in a Specac Model P/N 21000 Dewar assembly, with liquid N_2 or dry ice/acetone as coolant. The temperature of the cell was measured with a Cu–constantan thermocouple in contact with the inner window of the cell. Irradiations were effected with a Bausch and Lomb SP200 high-pressure Hg lamp filtered by a 10-cm H_2O filter with quartz windows and a Bausch and Lomb Model 33-86-79 high-intensity monochromator for 313-, 366-, and 436-nm irradiations. The 254-nm irradiations were effected with the unfiltered output from an Ultra-Violet Products Inc. Model PCQX1 low-pressure Hg lamp.

HPLC data were obtained with a HP 1084B HPLC equipped with a HP 1040A diode array detector. Compounds were identified on the basis of their retention times and UV–vis spectra, compared with those for authentic samples. The column used was a 15-cm Rainin Instruments Dynamax RP-C_{18} column. The eluent was a CH_3CN/H_2O gradient (80–100%).

Materials. All solvents were reagent or spectroscopic grade and were distilled and/or dried prior to use and stored over activated 3-Å molecular sieves. Methylcyclohexane (MCH) and 3-methylpentane (3MP) were distilled from Na under Ar and stored under Ar. Hexane and tetrahydrofuran (THF) were distilled from CaH_2 under N_2. Chlorinated solvents were freshly distilled from P_2O_5 under Ar and stored in the dark. MCH-d_{14} (Cambridge Isotope Laboratories) and CD_2Cl_2 (Aldrich) were used as received.

Silica gel for column chromatography was EM Science Keiselgel 60, 230–400 mesh. $Mn_2(CO)_{10}$ (Pressure Chemical) was sublimed prior to use. C_5Cl_6 (Aldrich), $Mn(CO)_5Cl$ (Strem), and $C_6H_5CH_2Br$ (Kodak) were used as received. 1-Bromopropane (Aldrich) and 1-iodobutane (Aldrich) were filtered through activated Al_2O_3 before use. Triphenylphosphine (Fluka) was recrystallized from C_2H_5OH and dried in vacuo. Bis(pentachlorocyclopentadienyl) was purchased from Aldrich; octachlorofulvalene was prepared by the literature technique.[20] All reactions and manipulations of organometallic compounds were carried out in a Vacuum Atmospheres drybox under Ar or on a conventional Schlenk line under Ar.

$(\eta^1\text{-}C_5Cl_5)Mn(CO)_5$ and $(\eta^5\text{-}C_5Cl_5)Mn(CO)_3$ were prepared by a previously reported technique[21] with the modification that the reaction mixture was chromatographed on silica gel with hexanes as the eluant. The first compound that eluted was $(\eta^5\text{-}C_5Cl_5)Mn(CO)_3$, and the second was $(\eta^1\text{-}C_5Cl_5)Mn(CO)_5$. Both compounds were recrystallized from pentane before use. Purity was assessed by HPLC, IR, melting point, and elemental analysis (Schwarzkopf Microanalytical Laboratories). Anal. Calcd for $\eta^1\text{-}C_5Cl_5)Mn(CO)_5$ (found): C, 27.78 (27.96); H, 0.00 (<0.06); Cl, 41.00 (41.06). Anal. Calcd for $(\eta^5\text{-}C_5Cl_5)Mn(CO)_3$ (found): C, 25.54 (25.36); H, 0.00 (<0.06); Cl, 47.11 (47.02).

$(\eta^1\text{-}C_6H_5CH_2)Mn(CO)_5$ was prepared by the method of Rausch[8] and the purity assessed by IR, NMR, and melting point. *cis*-$(\eta^1\text{-}C_6H_5CH_2)Mn(CO)_4PPh_3$ was prepared by the following procedure. A solution of 0.090 g of $(\eta^1\text{-}C_6H_5CH_2)Mn(CO)_5$ (3.14×10^{-4} mol, 1.57×10^{-3} M) and 0.10 g of PPh_3 (3.93×10^{-4} mol, 2.00×10^{-3} M) in 200 mL of Ar-purged hexane was irradiated at 0 °C with 254-nm light. The irradiation was monitored by IR spectroscopy and continued until the intensity of the starting material bands decreased by ~85%. The irradiation was then stopped, the solution filtered, and the solvent evaporated. The residue was chromatographed on silica gel (10% CH_2Cl_2 in C_6H_{14}). The PPh_3 adduct was obtained in 25% yield as pale yellow crystals. The ^1H NMR, IR, and mass spectra agree with the literature data.[22] Exact mass: (found) 520.0643 ± 0.0015, (calculated) 520.0636. Spectroscopic data for relevant compounds are included in Tables I and II.

Irradiations. Quantum yields were measured at 295 K under Ar or CO (1 atm) in deoxygenated MCH solutions with Hanovia medium-pressure Hg lamps with the appropriate solution and glass filters for 313, 366, and 436 nm and the unfiltered Ultra-Violet Products Inc. lamp for 254-nm light. Concentrations of starting materials and products were monitored by IR spectroscopy. Ferrioxalate actinometry[23] was used to

(7) Hudson, A.; Lappert, M. F.; Lednor, P. W.; Macquitty, J. J.; Nicholson, B. K. *J. Chem. Soc., Dalton Trans.* **1981**, 2159.
(8) Gismondi, T. E.; Rausch, M. D. *J. Organomet. Chem.* **1985**, *284*, 59.
(9) Miles, J. R.; Clark, R. J. *Inorg. Chem.* **1968**, *7*, 1801.
(10) Oliver, A. J.; Graham, W. A. G. *Inorg. Chem.* **1970**, *9*, 2578.
(11) Horton-Mastin, A.; Poliakoff, M.; Turner, J. J. *Organometallics* **1986**, *5*, 405.
(12) (a) Hitam, R. B.; Mahmoud, K. A.; Rest, A. J. *J. Organomet. Chem.* **1985**, *291*, 321. (b) Clarke, H. L.; Fitzpatrick, N. J. *J. Organomet. Chem.* **1972**, *40*, 379. (c) Davidson, G.; Andrews, D. C. *J. Chem. Soc., Dalton Trans.* **1972**, 126. (d) McClellan, W. R.; Hoehn, H. H.; Cripps, H. N.; Muetterties, E. L.; Howk, B. W. *J. Am. Chem. Soc.* **1961**, *83*, 1601.
(13) Collman, J. P.; Hegedus, L. S.; Norton, J. R.; Finke, R. G. *Principles and Applications of Organotransition Metal Chemistry*; University Science Books: Mill Valley, CA, 1987.
(14) Rest, A. J.; Whitwell, I.; Graham, W. A. G.; Hoyano, J. K.; McMaster, A. D. *J. Chem. Soc., Chem. Commun.* **1984**, 624.
(15) (a) Casey, C. P.; O'Connor, J. M.; Jones, W. D.; Haller, K. J. *Organometallics* **1983**, *2*, 535. (b) Rerek, M. E.; Basolo, F. *J. Am. Chem. Soc.* **1984**, *106*, 5908. (c) Schuster-Woldan, H. G.; Basolo, F. *J. Am. Chem. Soc.* **1966**, *88*, 5908.
(16) O'Connor, J. M.; Casey, C. P. *Chem. Rev.* **1987**, *87*, 307.
(17) (a) Crichton, O.; Rest, A. J.; Taylor, D. J. *J. Chem. Soc., Dalton Trans.* **1980**, 167. (b) Faller, J. W.; Crabtree, R. H.; Habib, A. *Organometallics* **1985**, *4*, 929. (c) Chetwynd-Talbot, J.; Gregenik, P.; Perutz, R. N.; Powell, M. H. A. *Inorg. Chem.* **1983**, *22*, 1675.
(18) (a) Huttner, G.; Brintzinger, H. H.; Bell, L. G.; Friedrich, P.; Bejenke, V.; Neugebauer, D. *J. Organomet. Chem.* **1978**, *145*, 329. (b) Nesmeyanov, A. N.; Ustynyuk, N. A.; Makarova, L. G. *J. Organomet. Chem.* **1978**, *159*, 189.
(19) Belmont, J. A.; Wrighton, M. S. *Organometallics* **1986**, *5*, 1421.
(20) Mark, V. *Org. Synth.* **1967**, *46*, 93.
(21) (a) Reimer, K. J.; Shaver, A. *Inorg. Synth.* **1980**, *XX*, 188. (b) Reimer, K. J.; Shaver, A. Inorg. *Chem.* **1975**, *14*, 2707.
(22) Drew, D.; Darensbourg, M. Y.; Darensbourg, D. J. *J. Organomet. Chem.* **1975**, *85*, 73.

Table I. IR and UV-Vis Spectroscopic Data For Relevant Compounds

compound[a]	T, K	IR (ν_{CO}) ($\epsilon \times 10^{-3}$)[b]	UV-vis ($\epsilon \times 10^{-4}$)[c]
$(\eta^1\text{-}C_5Cl_5)Mn(CO)_5$	295	2010 (4.7), 2041 (15.0), 2076 (0.44), 2126 (1.5)	290 (1.25), 212 (3.2)
	95	2009 (3.5), 2041 (11.0), 2031 (2.6), 2075 (0.52), 2127 (1.9)	
$(\eta^3\text{-}C_5Cl_5)Mn(CO)_4$	200	1959 (*4*), 2001 (*2*), 2020 (*5*), 2092 (*1*)	
	95	1963, 2004, 2018, 2093	
$(\eta^5\text{-}C_5Cl_5)Mn(CO)_3$	295	1980 (10.1), 2045 (5.8)	356 (0.08), 220 (3.0)
$(\eta^1\text{-}C_5Cl_5)Mn(CO)_4PPh_3$	295	1971 (*1*), 1998 (*2*), 2020 (*1*), 2082 (*1*)	
$Mn(CO)_5Cl$	295	1999 (5.2), 2054 (13.8), 2138	375 (0.06), 227 (1.3)
$Mn(CO)_5Br$	295	2007 (6.3), 2052 (16.5), 2138 (0.5)	
$Mn(CO)_5I$	295	2004 (4.5), 2045 (15.8), 2126 (1.0)	
$Mn_2(CO)_{10}$	295	1983 (7.8), 2014 (39.3), 2046 (12.2)	400 (0.6), 340 (3.5)
$Mn(CO)_5$[d]	295	1990	
$[Mn(CO)_4PPh_3]_2$[e]	295	1953 (14.0)	375 (3.0), 440 (0.6)
cis-$ClMn(CO)_4PPh_3$[e]	295	1958 (3.5), 2010 (4.2), 2030 (3.0), 2095 (2.4)	
$[Mn(CO)_4Cl]_2$	295	1977 (m), 2012 (m), 2045 (s), 2104 (w)	
$(\eta^1\text{-}C_3H_5)Mn(CO)_5$[f]	295	1988, 2012, 2048, 2109	
$(\eta^3\text{-}C_3H_5)Mn(CO)_4$[f]	295	1961, 1979, 1996, 2075	
$(\eta^1\text{-}C_6H_5CH_2)Mn(CO)_5$	295	1991 (6.3), 2009 (9.9), 2016 (10.0), 2043 (0.43), 2107 (1.3)	225 (2.0), 278 (1.2)
	95	1988 (4.9), 2006 (10.9), 2016 (10.3), 2044 (0.68), 2108 (1.6)	
$(\eta^3\text{-}C_6H_5CH_2)Mn(CO)_4$	295	1954 (*2.4*), 1976 (*3*), 1985 (*1.3*), 2065 (*1*)	
	95	1951 (9), 1975 (11), 1984 (2), 2066 (5.6)	390
cis-$(\eta^1\text{-}C_6H_5CH_2)Mn(CO)_4PPh_3$	295	1940 (2.5), 1966 (5.8), 1990 (2.7), 2053 (1.7)	218, 238
$C_{10}Cl_{10}$[g]	295	1251 (s), 1559 (w), 1596 (m)	240, 282, 324
$C_{10}Cl_8$[g]	295	1255, 1322, 1526	386, 590
C_5Cl_6[g]	295	1188 (w), 1231 (s), 1572 (w), 1606 (s)	320 (0.13)
$(\eta^5\text{-}C_5H_5)Fe(CO)_2Cl$[h]	295	2056 (3.7), 2004 (3.4)	
$[(\eta^5\text{-}C_5H_5)Fe(CO)_2]_2$[h]	295	2004 (3.0), 1960 (6.4), 1792 (6.2)	520 (0.8), 409 (2.1), 348 (8.3)

[a] All data recorded in alkane solution at 295 K except where noted. [b] Band positions in cm^{-1}. Extinction coefficients are in L mol^{-1} cm^{-1}. Italicized entries are relative extinction coefficients. [c] Band positions in nm. Extinction coefficients are in L mol^{-1} cm^{-1}. [d] Reference 25. [e] Reference 39. [f] Reference 12. [g] In CCl_4 solution at 295 K. [h] Reference 34.

Table II. NMR Spectroscopic Data for Relevant Compounds

compound[a]	^1H NMR, ppm	^{13}C NMR, ppm
$(\eta^1\text{-}C_5Cl_5)Mn(CO)_5$[b]		118, 205
$(\eta^5\text{-}C_5Cl_5)Mn(CO)_3$		94.7, 220
$(\eta^1\text{-}C_6H_5CH_2)Mn(CO)_5$[c]	7.11 (m, 4 H), 6.89 (t, 1 H) 2.34 (s, 2 H)	
$(\eta^3\text{-}C_6H_5CH_2)Mn(CO)_4$[c]	5.94 (m, 3 H),[d] 2.12 (s, 4 H)	
$(\eta^1\text{-}C_6H_5CH_2)Mn(CO)_4PPh_3$	7.6–7.2 (m, 15 H), 6.97 (m, 2 H), 6.89 (m, 2 H), 6.77 (m, 1 H), 1.62 (d, 2 H)	

[a] All spectra recorded at 295 K in CD_2Cl_2 except where noted. Peak positions reported downfield of TMS. [b] Reference 18. [c] Recorded at 200 K in MCH-d_{14} as solvent. [d] Broad.

measure the light intensity for each sample. Typical light intensities were 10^{-7}–10^{-8} einstein/min per cm^2.

Irradiations to determine qualitative aspects of the photochemistry were effected with Ar- or CO-purged alkane solutions containing approximately 10^{-3} M concentration of the metal carbonyl. The concentration of CO in MCH was measured by IR spectroscopy,[24] after the solution was cooled to 95 K, to be approximately 5×10^{-3} M. Irradiations were monitored by IR spectroscopy and typically carried to 5–10% conversion based on consumption of starting material.

^1H NMR spectra of $(\eta^1\text{-}C_6H_5CH_2)Mn(CO)_5$ and $(\eta^3\text{-}C_6H_5CH_2)Mn(CO)_4$ were measured at 200 K by placing a deoxygenated MCH-d_{14} solution of $(\eta^1\text{-}C_6H_5CH_2)Mn(CO)_5$ in a 5-mm quartz NMR tube in the cooled probe of the NMR spectrometer. After acquisition of an initial spectrum the sample was transferred to a quartz Dewar with dry ice/hexane as coolant. The NMR tube was then irradiated with 254-nm light and returned to the cooled NMR probe and a second spectrum obtained. UV-vis spectra were measured for the same sample by placing the NMR tube–Dewar assembly in the HP 8451A spectrometer.

Results

UV-Vis Absorption Spectra of $RMn(CO)_5$. The complexes studied show only tail absorptions in the visible region of the optical spectrum; $(\eta^1\text{-}C_5Cl_5)Mn(CO)_5$ is yellow, while $(\eta^1\text{-}C_6H_5CH_2)Mn(CO)_5$ is nearly colorless, Figure 1. $(\eta^1\text{-}C_5Cl_5)Mn(CO)_5$ shows maxima at 292 nm (ϵ = 12 500 M^{-1} cm^{-1}) and at 210 nm ($\epsilon \approx$ 38 000 M^{-1} cm^{-1}). It is worth noting that C_5Cl_6 shows a much weaker first absorption and at a somewhat lower energy, 323 nm (ϵ = 1300 M^{-1} cm^{-1}). $(\eta^1\text{-}C_6H_5CH_2)Mn(CO)_5$ has an absorption spectrum similar to that for the $\eta^1\text{-}C_5Cl_5$ complex with a first absorption at ~278 nm (ϵ = 12 000 M^{-1} cm^{-1}) and the second band at ~225 nm ($\epsilon \approx$ 20 000 M^{-1} cm^{-1}). From the absorption spectra it is evident that photochemical reactions could be possible from direct excitation with light in the high-energy region of the visible spectrum and in the near-ultraviolet. The spectra do not exhibit resolution of bands attributable to ligand field absorptions; presumably the O_h-like complexes have ligand field absorptions, but they are obscured by the more intense Mn → π^* CO charge-transfer bands.[1] The photochemical results, vide infra, are consistent with lowest excited states that involve population of the σ^*_z and σ^*_{xy} orbitals from the overlap of the Mn $3d_{z^2}$ and the $3d_{x^2-y^2}$ orbitals with the ligand-centered σ orbitals.

Photochemistry of $(\eta^1\text{-}C_5Cl_5)Mn(CO)_5$ at 95 K. CO Loss. Near-UV irradiation of $(\eta^1\text{-}C_5Cl_5)Mn(CO)_5$ in 3MP at 95 K results in rapid conversion of $(\eta^1\text{-}C_5Cl_5)Mn(CO)_5$ to the ring-slipped products $(\eta^3\text{-}C_5Cl_5)Mn(CO)_4$ and $(\eta^5\text{-}C_5Cl_5)Mn(CO)_3$ (eq 3 and 4). The ratio of η^3 to η^5 species formed upon photolysis

$$(\eta^1\text{-}C_5Cl_5)Mn(CO)_5 \xrightarrow{h\nu} (\eta^3\text{-}C_5Cl_5)Mn(CO)_4 + CO \quad (3)$$

$$(\eta^3\text{-}C_5Cl_5)Mn(CO)_4 \xrightarrow{h\nu \text{ or } \Delta} (\eta^5\text{-}C_5Cl_5)Mn(CO)_3 + CO \quad (4)$$

becomes smaller with increasing irradiation time, consistent with formation of the η^5 species via irradiation of the η^3 species. The growth of a four-band pattern in the IR at 1963, 2004, 2018, and 2093 cm^{-1} is associated with the formation of $(\eta^3\text{-}C_5Cl_5)Mn(CO)_4$, and the two bands at 2045 (obscured by starting material) and 1980 cm^{-1} are attributed to production of $(\eta^5\text{-}C_5Cl_5)Mn(CO)_3$, Figure 2. The relative positions and intensities of the four new bands assigned to the η^3 species correspond with the positions expected based on the related $(\eta^1\text{-}C_3H_5)Mn(CO)_5$ to $(\eta^3\text{-}C_3H_5)Mn(CO)_4$ conversion.[12] There are no features in the photoproduct spectrum at 95 K that can be assigned to the 16e $(\eta^1\text{-}C_5Cl_5)Mn(CO)_4$, which is presumably the prompt photoproduct resulting from CO loss. The bands assigned to $(\eta^5\text{-}C_5Cl_5)Mn(CO)_3$ are identical with those for an authentic sample recorded in the same medium. The absorbance[24] for free CO at 2132 cm^{-1} is obscured by the starting material; higher conversions do show free CO but only when it is obvious that secondary

(23) Murov, S. L. *Handbook of Photochemistry*; Marcel Dekker: New York, 1973.
(24) Pope, K. R.; Wrighton, M. S. *Inorg. Chem.* **1985**, *24*, 2792.

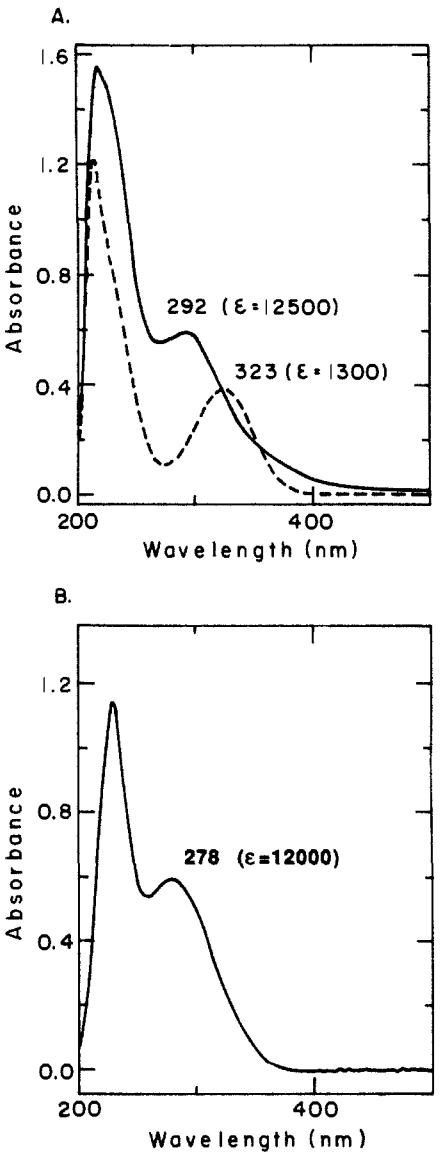

Figure 1. UV-vis absorption spectra: (A) for $(\eta^1\text{-}C_5Cl_5)Mn(CO)_5$ (5×10^{-5} M, —) and C_5Cl_6 (3×10^{-4} M, ---) in hexane at 295 K (note that the concentrations of the two are not the same); (B) for $(\eta^1\text{-}C_6H_5CH_2)Mn(CO)_5$ (5×10^{-5} M) in hexane at 295 K.

photochemistry is occurring. In the 3MP matrix the chemical yields of $(\eta^5\text{-}C_5Cl_5)Mn(CO)_3$ and $(\eta^3\text{-}C_5Cl_5)Mn(CO)_4$ are ~80% and ~20%, respectively, at ~25% consumption of $(\eta^1\text{-}C_5Cl_5)Mn(CO)_5$. No IR absorbances for $Mn(CO)_5$, Table I, are observed upon irradiation of $(\eta^1\text{-}C_5Cl_5)Mn(CO)_5$ in a matrix, indicating that no net Mn–R bond cleavage occurs under such conditions.[25]

When a matrix containing $(\eta^3\text{-}C_5Cl_5)Mn(CO)_4$ is warmed to 295 K, there is regeneration of $(\eta^1\text{-}C_5Cl_5)Mn(CO)_5$ (85%) and additional formation of $(\eta^5\text{-}C_5Cl_5)Mn(CO)_3$ (15%). Such warmup experiments show that conversion of $(\eta^3\text{-}C_5Cl_5)Mn(CO)_4$ to $(\eta^5\text{-}C_5Cl_5)Mn(CO)_3$ can be a thermal process (eq 5) that can occur

$$(\eta^3\text{-}C_5Cl_5)Mn(CO)_4 \xrightarrow{\Delta} (\eta^5\text{-}C_5Cl_5)Mn(CO)_3 + CO \quad (5)$$

$$(\eta^3\text{-}C_5Cl_5)Mn(CO)_4 \rightleftharpoons (\eta^1\text{-}C_5Cl_5)Mn(CO)_4 \quad (6)$$

$$(\eta^1\text{-}C_5Cl_5)Mn(CO)_4 + CO \xrightarrow{\Delta} (\eta^1\text{-}C_5Cl_5)Mn(CO)_5 \quad (7)$$

competitively with back-reaction with CO to regenerate the

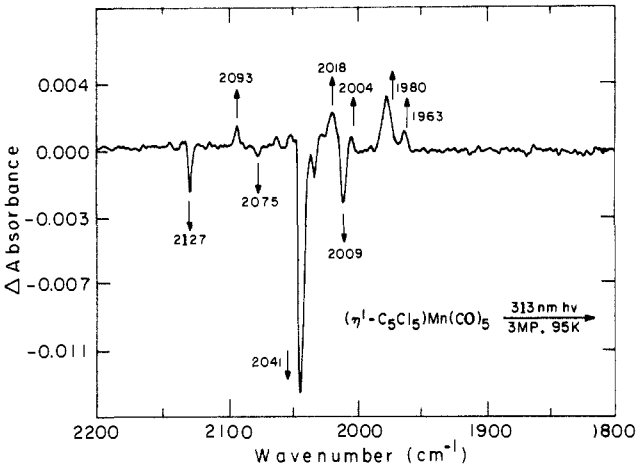

Figure 2. IR difference spectrum resulting from 313-nm irradiation of $(\eta^1\text{-}C_5Cl_5)Mn(CO)_5$ in a 3MP matrix at 95 K. Negative peaks are due to consumption of starting material. Positive peaks at 2093, 2018, 2004, and 1963 cm^{-1} are due to $(\eta^3\text{-}C_5Cl_5)Mn(CO)_4$. The peak at 1980 cm^{-1} is due to formation of $(\eta^5\text{-}C_5Cl_5)Mn(CO)_3$ (a second peak for $(\eta^5\text{-}C_5Cl_5)Mn(CO)_3$ at 2045 cm^{-1} is obscured by starting material).

pentacarbonyl. The regeneration of $(\eta^1\text{-}C_5Cl_5)Mn(CO)_5$ likely occurs via the processes represented by eq 6 and 7. Thermal conversion of $(\eta^3\text{-}C_5Cl_5)Mn(CO)_4$ to $(\eta^5\text{-}C_5Cl_5)Mn(CO)_3$ (eq 5) has been monitored quantitatively at 220 K. We find the rate to be 1×10^{-4} s^{-1}. However, at 95 K the thermal chemistry is negligibly slow, and $(\eta^5\text{-}C_5Cl_5)Mn(CO)_3$ apparently forms via photoexcitation of $(\eta^3\text{-}C_5Cl_5)Mn(CO)_4$ (eq 4).

As in a 3MP matrix, irradiation of $(\eta^1\text{-}C_5Cl_5)Mn(CO)_5$ in a MCH matrix at 95 K also results in the formation of $(\eta^5\text{-}C_5Cl_5)Mn(CO)_3$ and $(\eta^3\text{-}C_5Cl_5)Mn(CO)_4$, but accumulation of the η^3 species is less significant (~10% versus ~20% at 25% consumption of $(\eta^1\text{-}C_5Cl_5)Mn(CO)_5$). The $(\eta^3\text{-}C_5Cl_5)Mn(CO)_4$ formed from $(\eta^1\text{-}C_5Cl_5)Mn(CO)_5$ is obviously photosensitive in alkane matrices, and less accumulates in the harder MCH matrix compared to the softer 3MP matrix. The same photoproducts are found in low-temperature (95 K) but fluid, alkane solution (isopentane/cyclopentane, 4:1):[26] that is formation of $(\eta^3\text{-}C_5Cl_5)Mn(CO)_4$ and $(\eta^5\text{-}C_5Cl_5)Mn(CO)_3$ results and the ratio of these products decreases with increasing irradiation time. However, higher conversion of $(\eta^1\text{-}C_5Cl_5)Mn(CO)_5$ to $(\eta^3\text{-}C_5Cl_5)Mn(CO)_4$ (~50% at 25% consumption of $(\eta^1\text{-}C_5Cl_5)Mn(CO)_5$) occurs in the fluid medium compared to rigid media. The higher chemical yield of the $(\eta^3\text{-}C_5Cl_5)Mn(CO)_4$ in fluid media suggests that back-reaction of the 16e $(\eta^3\text{-}C_5Cl_5)Mn(CO)_3$ with CO might be competitive with ring slippage to give $(\eta^5\text{-}C_5Cl_5)Mn(CO)_3$.

Photochemistry of $(\eta^1\text{-}C_5Cl_5)Mn(CO)_5$ at 200 K. Competitive CO Loss and Radical Chemistry. Irradiation of $(\eta^1\text{-}C_5Cl_5)Mn(CO)_5$ in fluid, deoxygenated alkane solutions at 200 K gives a significant yield of $Mn(CO)_5Cl$ in addition to $(\eta^5\text{-}C_5Cl_5)Mn(CO)_3$ and $(\eta^3\text{-}C_5Cl_5)Mn(CO)_4$, Figure 3. As in the 95 K irradiations the ratio of η^3 to η^5 CO-loss products declines with increasing irradiation time, consistent with $(\eta^5\text{-}C_5Cl_5)Mn(CO)_3$ formation via photoexcitation of $(\eta^3\text{-}C_5Cl_5)Mn(CO)_4$. $(\eta^3\text{-}C_5Cl_5)Mn(CO)_4$ is essentially thermally inert at 200 K, with no appreciable thermal reaction after several hours in the dark. Both $(\eta^5\text{-}C_5Cl_5)Mn(CO)_3$ and $Mn(CO)_5Cl$ are photosensitive, but no products derived from photolysis of $(\eta^5\text{-}C_5Cl_5)Mn(CO)_3$ or $Mn(CO)_5Cl$ are observed at sufficiently low extent consumption (<10%) of $(\eta^1\text{-}C_5Cl_5)Mn(CO)_5$. Much higher conversions to $(\eta^3\text{-}C_5Cl_5)Mn(CO)_4$ are possible (~50% at 25% consumption at $(\eta^1\text{-}C_5Cl_5)Mn(CO)_5$) for irradiation of $(\eta^1\text{-}C_5Cl_5)Mn(CO)_5$ at 200 K in fluid solutions than in a rigid alkane matrix at 95 K, consistent with the photochemistry in fluid solution at 95 K. Warming of the photoproduct mixture formed at 200 K to 295 K results in the formation of

(25) (a) Church, S. P.; Hermann, H.; Grevels, F.-W.; Schaffner, K. *J. Chem. Soc., Chem. Commun.* **1984**, 785. (b) Hepp, A. F.; Wrighton, M. S. *J. Am. Chem. Soc.* **1983**, *105*, 5934.

(26) Casal, H. L.; McGimpsey, W. G.; Scaiano, J. C.; Bliss, R. A.; Sauers, R. R. *J. Am. Chem. Soc.* **1986**, *108*, 8255.

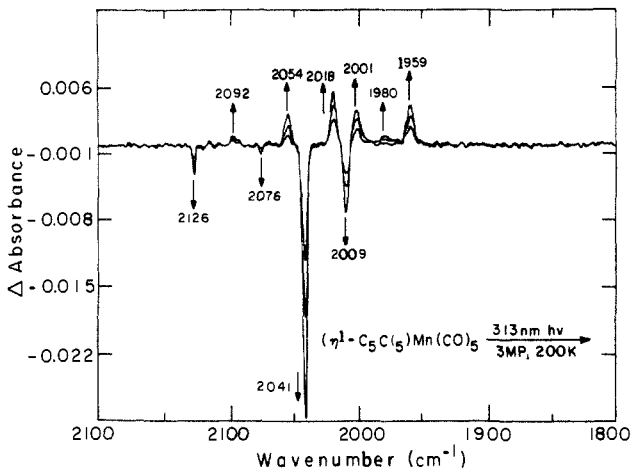

Figure 3. Sequential IR difference spectra resulting from 313-nm irradiation of (η^1-C_5Cl_5)Mn(CO)$_5$ in a 3MP solution at 200 K for 20-, 40-, and 60-s irradiation times. Negative peaks are due to consumption of starting material. Positive peaks at 2092, 2018, 2001, and 1959 cm^{-1} are due to (η^3-C_5Cl_5)Mn(CO)$_4$. The peak at 2054 cm^{-1} is due to Mn(CO)$_5$Cl, and the peak at 1980 cm^{-1} is due to (η^5-C_5Cl_5)Mn(CO)$_3$. The peak at 2045 (for (η^5-C_5Cl_5)Mn(CO)$_3$) is obscured by starting material. The peak at 1999 cm^{-1} (for Mn(CO)$_5$Cl) overlaps the ~2001-cm^{-1} absorption of (η^2-C_5Cl_5)Mn(CO)$_4$.

(η^1-C_5Cl_5)Mn(CO)$_5$ and (η^5-C_5Cl_5)Mn(CO)$_3$ from the η^3 species with a typical ratio of 5 to 1.

Compared to the 95 K results, the significant finding from irradiation of (η^1-C_5Cl_5)Mn(CO)$_5$ at 200 K is that Mn(CO)$_5$Cl is formed in significant yield. The Mn(CO)$_5$Cl presumably arises from homolysis according to eq 2 to give the Mn(CO)$_5$ radical that abstracts Cl from a molecule of starting material or from the C_5Cl_5 released in the primary homolysis. We do find that the three metal carbonyl products observed, (η^3-C_5Cl_5)Mn(CO)$_4$, (η^5-C_5Cl_5)Mn(CO)$_3$, and Mn(CO)$_5$Cl, only account for ~70% of the (η^1-C_5Cl_5)Mn(CO)$_5$ consumed, consistent with reaction of photogenerated Mn(CO)$_5$ with a second molecule of starting material (eq 8 and 9). Room-temperature experiments (vide

$$(\eta^1\text{-}C_5Cl_5)Mn(CO)_5 \xrightarrow{h\nu} Mn(CO)_5 + C_5Cl_5 \qquad (8)$$

$$Mn(CO)_5 + (\eta^1\text{-}C_5Cl_5)Mn(CO)_5 \xrightarrow{\Delta} Mn(CO)_5Cl + \text{unidentified products} \qquad (9)$$

infra) support the hypothesis represented by eq 8 and 9. The ratio of Mn(CO)$_5$Cl to products derived from CO loss, (η^3-C_5Cl_5)Mn(CO)$_4$ and (η^5-C_5Cl_5)Mn(CO)$_3$, is wavelength dependent. Lower energy irradiation (366 nm) produces approximately 20% Mn(CO)$_5$Cl, while higher energy irradiation (254 nm) yields almost exclusively the CO-loss products (η^3-C_5Cl_5)Mn(CO)$_4$ and (η^5-C_5Cl_5)Mn(CO)$_3$.

Irradiation of (η^1-C_5Cl_5)Mn(CO)$_5$ at 200 K in the presence of 2e-donor ligands has been carried out, in order to explore the reactivity of the presumed primary CO-loss product, the 16e (η^1-C_5Cl_5)Mn(CO)$_4$, which has not been detected at 95 K. Irradiation of (η^1-C_5Cl_5)Mn(CO)$_5$ at 200 K in MCH containing 0.5 or 3.0 M 1-pentene does not affect the distribution of the three metal carbonyl products at a given extent consumption of (η^1-C_5Cl_5)Mn(CO)$_5$. Specifically, no features attributable to (η^1-C_5Cl_5)Mn(CO)$_4$(pentene) are seen in the IR spectra of photoproduct mixtures. This result is consistent with the conclusion that intramolecular trapping of the 16e (η^1-C_5Cl_5)Mn(CO)$_4$ by an uncoordinated double bond of the η^1-cyclopentadienyl ring yields a more stable product than the product derived from intermolecular trapping by 1-pentene. It is also possible, of course, that 1-pentene simply does not compete for the open site even at 3.0 M. Irradiation at 200 K of (η^1-C_5Cl_5)Mn(CO)$_5$ in MCH containing ~5 mM CO also gives (η^3-C_5Cl_5)Mn(CO)$_4$, (η^5-C_5Cl_5)Mn(CO)$_3$, and Mn(CO)$_5$Cl. However, there is a decrease in the ratio of the CO-loss products to Mn(CO)$_5$Cl of ~60% at the same extent conversion following 313-nm irradiation as compared to irradiation in the absence of added CO. This result is consistent with the conclusion that (η^1-C_5Cl_5)Mn(CO)$_4$ generated in the primary photoprocess can be trapped by CO to regenerate (η^1-C_5Cl_5)Mn(CO)$_5$. The suppression of CO-loss products is not due to the thermal process represented by eq 6 and 7, because the (η^3-C_5Cl_5)Mn(CO)$_4$ is thermally inert at 200 K on the time scale of the photoreaction and sample analysis.

To further explore the reactivity of the primary 16e (η^1-C_5Cl_5)Mn(CO)$_4$ photoproduct, trapping reactions with PPh$_3$ were examined. Irradiation of (η^1-C_5Cl_5)Mn(CO)$_5$ in alkane solution containing 0.1 M PPh$_3$ at 200 K gives a mixture of primary photoproducts. The product derived from radical formation is *cis*-ClMn(CO)$_4$PPh$_3$, expected on the basis of known[1] processes of Mn(CO)$_5$ radicals in the presence of PPh$_3$ and Cl atom donors. The products from light-induced CO loss from (η^1-C_5Cl_5)Mn(CO)$_5$ include (η^5-C_5Cl_5)Mn(CO)$_3$, (η^3-C_5Cl_5)Mn(CO)$_4$, and (η^1-C_5Cl_5)Mn(CO)$_4$PPh$_3$, which has four IR bands at 2082, 2020, 1998, and 1971 cm^{-1}. The PPh$_3$ photosubstitution product is assigned on the basis of IR band positions and intensities compared to known RMn(CO)$_4$PPh$_3$ species. The initial yield of (η^3-C_5Cl_5)Mn(CO)$_4$ is attenuated by the presence of PPh$_3$, presumably due to trapping of the primary photoproduct, the 16e (η^1-C_5Cl_5)Mn(CO)$_4$ to form *cis*-(η^1-C_5Cl_5)Mn(CO)$_4$PPh$_3$. The initial (within 45 s) ratio of (η^3-C_5Cl_5)Mn(CO)$_4$ and *cis*-(η^1-C_5Cl_5)Mn(CO)$_4$PPh$_3$ is 4:1, but within ~20 min the (η^3-C_5Cl_5)Mn(CO)$_4$ reacts completely to give only *cis*-(η^1-C_5Cl_5)Mn(CO)$_4$PPh$_3$. Likewise, warming an initial photoproduct mixture to 295 K results in very rapid consumption of (η^3-C_5Cl_5)Mn(CO)$_4$ to form only additional *cis*-(η^1-C_5Cl_5)Mn(CO)$_4$PPh$_3$. *cis*-(η^1-C_5Cl_5)Mn(CO)$_4$PPh$_3$ is thermally inert at 295 K.

The photochemistry of (η^1-C_5Cl_5)Mn(CO)$_5$ in the presence of PPh$_3$ shows that the prompt CO-loss product can be scavenged by PPh$_3$ (eq 10 and 11). The thermal chemistry of (η^3-

$$(\eta^1\text{-}C_5Cl_5)Mn(CO)_5 \xrightarrow{h\nu} (\eta^1\text{-}C_5Cl_5)Mn(CO)_4 + CO \qquad (10)$$

$$(\eta^1\text{-}C_5Cl_5)Mn(CO)_4 + L \xrightarrow{\Delta} (\eta^1\text{-}C_5Cl_5)Mn(CO)_4L \qquad (11)$$

C_5Cl_5)Mn(CO)$_4$ is likely due to the competitive processes shown in eq 5 and 6. Since thermal reaction of (η^3-C_5Cl_5)Mn(CO)$_4$ in the presence of 0.1 M PPh$_3$ yields only (η^1-C_5Cl_5)Mn(CO)$_4$PPh$_3$, and not (η^5-C_5Cl_5)Mn(CO)$_3$, at 200 K or upon warming to 295 K it appears that the thermal $\eta^3 \rightarrow \eta^1$ conversion in eq 6 to open a coordination site must be more rapid than the thermal $\eta^3 \rightarrow \eta^5$ conversion in eq 5.

Room-Temperature Photochemistry of (η^1-C_5Cl_5)Mn(CO)$_5$. Irradiation of (η^1-C_5Cl_5)Mn(CO)$_5$ in deoxygenated alkane solvents at 295 K produces mainly two compounds, (η^5-C_5Cl_5)Mn(CO)$_3$ and Mn(CO)$_5$Cl, which account for typically only 70% of the (η^1-C_5Cl_5)Mn(CO)$_5$ consumed; trace amounts of $Mn_2(CO)_{10}$ are observed, but no other metal carbonyl products are observed by IR or HPLC analysis of the irradiated mixture. The ratio of these products shows the same qualitative wavelength dependence as is observed at 200 K, Figure 4: More CO-loss chemistry is observed at shorter excitation wavelengths. Irradiation of (η^1-C_5Cl_5)Mn(CO)$_5$ at 366 or 436 nm in alkane solution containing 0.5 M 1-bromopentane or 1-iodobutane results in the complete suppression of Mn(CO)$_5$Cl formation, and Mn(CO)$_5$Br or Mn(CO)$_5$I, respectively, is formed as the principal metal carbonyl derived from loss of C_5Cl_5. In the presence of either halide donor, the (η^5-C_5Cl_5)Mn(CO)$_3$ and Mn(CO)$_5$X (X = Br, I) formed typically account for ~85% of the (η^1-C_5Cl_5)Mn(CO)$_5$ consumed. The amount of (η^5-C_5Cl_5)Mn(CO)$_3$ formed is unaffected by the added 0.5 M alkyl halide. At alkyl halide concentrations significantly lower than 0.5 M both Mn(CO)$_5$Cl and Mn(CO)$_5$X (X = Br, I) are formed. Irradiation of (η^1-C_5Cl_5)Mn(CO)$_5$ in alkane solution containing O_2 results in the formation of (η^5-C_5Cl_5)Mn(CO)$_3$ in the typical yield (~70% of consumed (η^1-C_5Cl_5)Mn(CO)$_5$ following 366-nm irradiation), but no Mn(CO)$_5$Cl is detected.

HPLC analysis of a photoproduct mixture produced by 366-nm irradiation at 295 K of (η^1-C_5Cl_5)Mn(CO)$_5$ shows formation of bis(pentachlorocyclopentadienyl), $C_{10}Cl_{10}$, as the major product

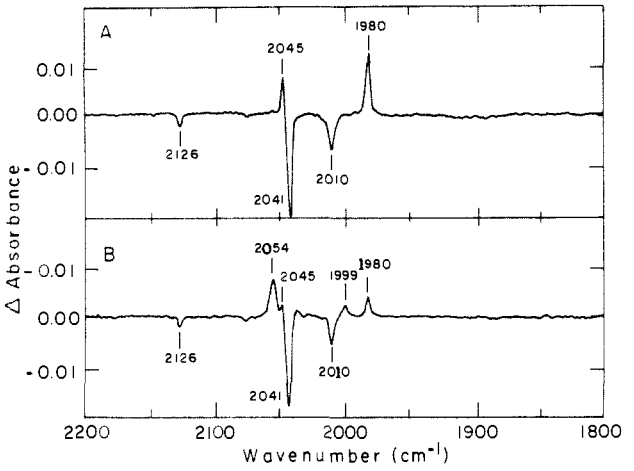

Figure 4. IR difference spectra resulting from irradiation of $(\eta^1\text{-}C_5Cl_5)Mn(CO)_5$ in a 3MP solution at 295 K: (A) IR spectral changes upon 254-nm irradiation. Negative peaks are due to consumption of starting material, and positive peaks are due to formation of $(\eta^5\text{-}C_5Cl_5)Mn(CO)_3$. (B) IR spectral changes resulting from 436-nm irradiation. Negative peaks are due to consumption of starting material. Positive peaks at 2045 and 1980 cm^{-1} are due to formation of $(\eta^5\text{-}C_5Cl_5)Mn(CO)_3$. Positive peaks at 2054 and 1999 cm^{-1} are due to formation of $Mn(CO)_5Cl$.

Table III. Quantum Yields for $(\eta^1\text{-}C_5Cl_5)Mn(CO)_5$ Photolyses[a]

	Φ_{dis}		Φ_{-CO}		$\Phi_{homolysis}$[b]	
λ, nm	Ar	CO[c]	Ar	CO	Ar	CO
254	0.41	0.11	0.30	0.08	0.04	0.03
313	0.31	0.13	0.15	0.02	0.06	0.04
366	0.15	0.08	0.04	0.004	0.06	0.05
436	0.13	0.08	0.03	$<10^{-3}$	0.06	0.05

[a] Irradiations were effected in 3.0 mL of deoxygenated MCH solutions using a merry-go-round and ferrioxalate actinometry to determine the excitation rate. Quantum yields are ±10%. [b] Determined from the ratio of $Mn(CO)_5Cl$ formed to $(\eta^1\text{-}C_5Cl_5)Mn(CO)_5$ consumed in separate photolyses in CaF_2 IR cells. [c] Typical CO concentrations are ~5 mM as measured by IR spectroscopy.

derived from the C_5Cl_5 fragment. The $C_{10}Cl_{10}$ accounts for ~70% of the C_5Cl_5. No evidence for octachlorofulvalene, $C_{10}Cl_8$, formation was observed by HPLC.

The Cl atom source to yield $Mn(CO)_5Cl$ from irradiation of $(\eta^1\text{-}C_5Cl_5)Mn(CO)_5$ in the absence of added alkyl halides is believed to be a second molecule of $(\eta^1\text{-}C_5Cl_5)Mn(CO)_5$ (eq 8 and 9). However, the product derived from abstraction of Cl from $(\eta^1\text{-}C_5Cl_5)Mn(CO)_5$ by $Mn(CO)_5$ has not been observed. Irradiation at $\lambda > 500$ nm of $[(\eta^5\text{-}C_5H_5)Fe(CO)_2]_2$ in an alkane solution containing 10^{-3} M $(\eta^1\text{-}C_5Cl_5)Mn(CO)_5$ results in consumption of both $[(\eta^5\text{-}C_5H_5)Fe(CO)_2]_2$ and $(\eta^1\text{-}C_5Cl_5)Mn(CO)_5$ in the ratio 1:1.3. Since $(\eta^1\text{-}C_5Cl_5)Mn(CO)_5$ does not absorb $\lambda > 500$ nm light, the primary photoreaction is presumably generation of $(\eta^5\text{-}C_5H_5)Fe(CO)_2$.[1] A total of 1.9 ± 0.2 molecules of $(\eta^5\text{-}C_5H_5)Fe(CO)_2Cl$ was formed for each $[(\eta^5\text{-}C_5H_5)Fe(CO)_2]_2$ consumed, as well as a second, but minor, product with IR bands at 2121 (w), 2064 (vw), 2031 (s), 2027 (s), 2002 (m), and 1997 (m) cm^{-1}. The compound with these six IR bands is believed to be the radical coupling product from $(\eta^5\text{-}C_5H_5)Fe(CO)_2$ and $(\eta^1\text{-}C_5Cl_4)Mn(CO)_5$; work to isolate this compound is under way. At least this experiment shows that $(\eta^1\text{-}C_5Cl_5)Mn(CO)_5$ can serve as a Cl atom donor toward a metal-centered radical. That fewer than two molecules of $(\eta^1\text{-}C_5Cl_5)Mn(CO)_5$ are consumed for every $(\eta^5\text{-}C_5H_5)Fe(CO)_2$ generated is consistent with the conclusion that a molecule of $(\eta^1\text{-}C_5Cl_5)Mn(CO)_5$ can potentially serve as a donor of more than one Cl atom.

Quantum yields at 295 K for the disappearance of $(\eta^1\text{-}C_5Cl_5)Mn(CO)_5$ and the appearance of $(\eta^5\text{-}C_5Cl_5)Mn(CO)_3$ and $Mn(CO)_5Cl$ were measured in the presence of both Ar and CO, Table III. The data show that the quantum yield for the radical pathway is relatively insensitive to excitation wavelength, whereas

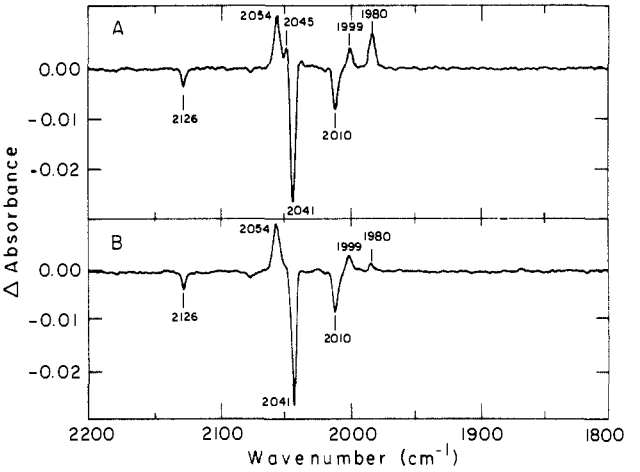

Figure 5. IR spectral changes accompanying 313-nm irradiation of $(\eta^1\text{-}C_5Cl_5)Mn(CO)_5$ at 295 K: (A) changes following irradiation in Ar-deoxygenated MCH; (B) changes following irradiation in CO-deoxygenated MCH. The negative bands are due to consumption of starting material. The peaks at 2045 and 1980 cm^{-1} are due to formation of $(\eta^5\text{-}C_5Cl_5)Mn(CO)_3$, and the peaks at 2054 and 1999 cm^{-1} are due to formation of $Mn(CO)_5Cl$.

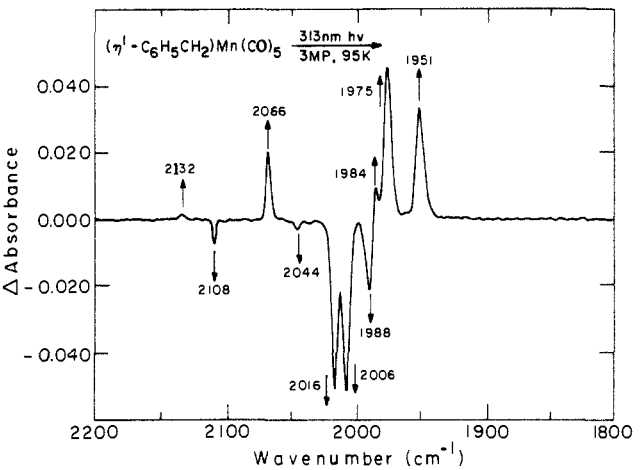

Figure 6. IR difference spectra accompanying 313-nm irradiation of $(\eta^1\text{-}C_6H_5CH_2)Mn(CO)_5$ in a 3MP matrix at 95 K. The negative peaks are due to consumption of starting material. The peak at 2132 cm^{-1} is due to free CO in the matrix. Positive peaks at 2066, 1984, 1975, and 1951 cm^{-1} are due to formation of $(\eta^3\text{-}C_6H_5CH_2)Mn(CO)_4$.

the CO-loss chemistry is strongly wavelength dependent. Added CO suppresses the formation of $(\eta^5\text{-}C_5Cl_5)Mn(CO)_3$ and the disappearance of $(\eta^1\text{-}C_5Cl_5)Mn(CO)_5$ at all wavelengths but has little effect on the formation of the radical-derived product $Mn(CO)_5Cl$, Figure 5. Interestingly, the effect of added CO on the reaction depends on wavelength. The suppression of CO-loss chemistry is more effective for long-wavelength excitation than for that at short wavelengths. The disappearance quantum yield of $(\eta^1\text{-}C_5Cl_5)Mn(CO)_5$ was also measured at 366 nm in an Ar-purged alkane solution containing 0.1 M PPh_3. The disappearance quantum yield of $(\eta^1\text{-}C_5Cl_5)Mn(CO)_5$ is 0.13, essentially unchanged from the 0.15 measured in the absence of PPh_3. Thus, the presence of PPh_3 does not affect the rate of consumption of $(\eta^1\text{-}C_5Cl_5)Mn(CO)_5$, but of course, the products include *cis*-$(\eta^1\text{-}C_5Cl_5)Mn(CO)_4PPh_3$ and *cis*-$ClMn(CO)_4PPh_3$. The appearance quantum yield of $(\eta^5\text{-}C_5Cl_5)Mn(CO)_3$ is 0.01, decreased from the 0.04 observed in the absence of PPh_3. This decrease in the efficiency of formation of $(\eta^5\text{-}C_5Cl_5)Mn(CO)_3$ is due to the trapping of the presumed intermediate $(\eta^3\text{-}C_5Cl_5)Mn(CO)_4$ by PPh_3 to form *cis*-$(\eta^1\text{-}C_5Cl_5)Mn(CO)_4PPh_3$.

Low-Temperature Photochemistry of $(\eta^1\text{-}C_6H_5CH_2)Mn(CO)_5$. Irradiation of $(\eta^1\text{-}C_6H_5CH_2)Mn(CO)_5$ at 254, 313, or 366 nm in a MCH matrix at 95 K leads to a decrease in the intensity of IR bands for $(\eta^1\text{-}C_6H_5CH_2)Mn(CO)_5$ and growth of four new

bands at 1951, 1975, 1984, and 2066 cm^{-1}. In addition, the absorbance of free CO is observed at 2132 cm^{-1}, Figure 6. From the extinction coefficient for free CO,[24] we calculate that 0.92 ± 0.06 molecule of CO is produced for every molecule of (η^1-$C_6H_5CH_2$)$Mn(CO)_5$ consumed. The photoproduct is photostable in a MCH matrix at 95 K, and essentially quantitative (>95%) conversion of (η^1-$C_6H_5CH_2$)$Mn(CO)_5$ to the new complex can be effected with no secondary photochemistry detected by IR. On the basis of the similarity of the relative positions and intensities of the CO stretching bands of this new complex to those in (η^3-C_5Cl_5)$Mn(CO)_4$ and (η^3-C_3H_5)$Mn(CO)_4$,[12] we assign the structure of the photoproduct to be (η^3-$C_6H_5CH_2$)$Mn(CO)_4$ (eq 12). We find no spectroscopic evidence for the presumed 16e

$$(\eta^1\text{-}C_6H_5CH_2)Mn(CO)_5 \xrightarrow[-CO]{h\nu} [(\eta^1\text{-}C_6H_5CH_2)Mn(CO)_4] \xrightarrow{\Delta} (\eta^3\text{-}C_6H_5CH_2)Mn(CO)_4 \quad (12)$$

species (η^1-$C_6H_5CH_2$)$Mn(CO)_4$. Trapping reactions with CO and PPh_3 and spectroscopic data at 200 K are also consistent with formulation of the photoproduct as (η^3-$C_6H_5CH_2$)$Mn(CO)_4$. Warmup of the irradiation mixture containing the (η^3-$C_6H_5CH_2$)$Mn(CO)_4$ to 295 K results in the disappearance of the η^3 species with quantitative (>95%) regeneration of (η^1-$C_6H_5CH_2$)$Mn(CO)_5$. If the warmup is effected in the presence of 0.1 M PPh_3, a new four-band pattern assigned to *cis*-η^1-$C_6H_5CH_2$)$Mn(CO)_4PPh_3$ at 1940, 1966, 1990, and 2053 cm^{-1} grows and no regeneration of (η^1-$C_6H_5CH_2$)$Mn(CO)_5$ is found (eq 13). These four bands are identical with those observed in the IR spectrum of authentic *cis*-(η^1-$C_6H_5CH_2$)$Mn(CO)_4PPh_3$, Table I.

$$(\eta^3\text{-}C_6H_5CH_2)Mn(CO)_4 \overset{\Delta}{\rightleftharpoons} [(\eta^1\text{-}C_6H_5CH_2)Mn(CO)_4] \xrightarrow{+L} (\eta^1\text{-}C_6H_5CH_2)Mn(CO)_4L \ (L = CO, PPh_3) \quad (13)$$

254-nm irradiation of (η^1-$C_6H_5CH_2$)$Mn(CO)_5$ in Ar-purged alkane solutions at 200 K results in the clean formation of only (η^3-$C_6H_5CH_2$)$Mn(CO)_4$. Irradiation (313 or 366 nm) at 200 K of (η^1-$C_6H_5CH_2$)$Mn(CO)_5$ in deoxygenated alkane results in the formation of both (η^3-$C_6H_5CH_2$)$Mn(CO)_4$ (95% following 313-nm excitation) and $Mn_2(CO)_{10}$ (5% following 313-nm excitation). If the alkane contains 0.1 M CCl_4, then both (η^3-$C_6H_5CH_2$)$Mn(CO)_4$ and $Mn(CO)_5Cl$ are formed and the formation of $Mn_2(CO)_{10}$ is not found. As in the case of R = C_5Cl_5, the ratio of CO loss to Mn–R bond homolysis is wavelength dependent for R = $CH_2C_6H_5$. Low-energy irradiation, 366 nm, yields 45% of products derived from Mn–R bond homolysis, while irradiation at 313 nm leads to preferential CO loss, with only 5% of the (η^1-$C_6H_5CH_2$)$Mn(CO)_5$ being converted to $Mn(CO)_5Cl$, Figure 7.

(η^3-$C_6H_5CH_2$)$Mn(CO)_4$ produced by 254-nm irradiation of (η^1-$C_6H_5CH_2$)$Mn(CO)_5$ in Ar-deoxygenated MCH-d_{14} at 200 K can be detected by ^1H NMR. Upon irradiation the proton resonances for (η^1-$C_6H_5CH_2$)$Mn(CO)_5$ decline and there is growth of a new resonance at 2.12 ppm that integrates to four protons and a new broad multiplet at 5.94 ppm that integrates to three protons. Concurrent with these changes in the ^1H NMR, the sample becomes intensely yellow with growth of an absorbance maximum at 390 nm, which tails into the visible region. The new resonances at 5.94 ppm are assigned to protons H_A, similar to the vinyl proton resonance of 1,3-cyclohexadiene at 5.86 ppm,[27] and the resonance at 2.12 ppm is assigned to the allyl-like protons H_B of (η^3-$C_6H_5CH_2$)$Mn(CO)_4$.[13,28] These new proton resonances are similar to those observed for other η^3-$C_6H_5CH_2$ complexes at temperatures where the complexes are fluxional.[29] Since only two new resonances are observed for (η^3-$C_6H_5CH_2$)$Mn(CO)_4$, we

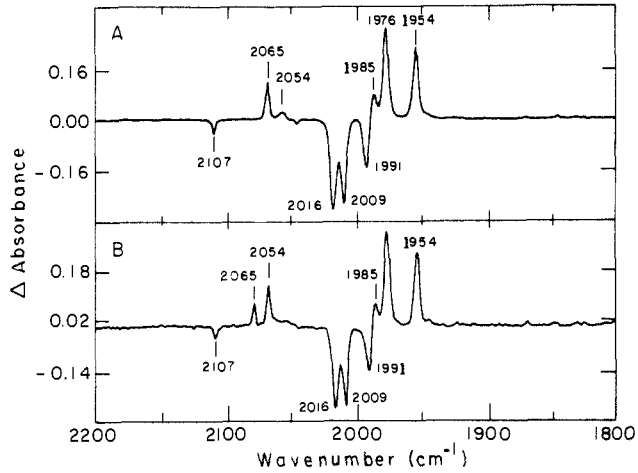

Figure 7. IR spectral changes accompanying irradiation of (η^1-$C_6H_5CH_2$)$Mn(CO)_5$ at 200 K in MCH containing 0.1 M CCl_4: (A) changes upon 313-nm irradiation; (B) changes upon 366-nm irradiation. Negative peaks are due to consumption of starting material. Positive peaks at 2065, 1985, 1976, and 1954 cm^{-1} are due to formation of (η^3-$C_6H_5CH_2$)$Mn(CO)_4$. The peak at 2054 cm^{-1} is due to formation of $Mn(CO)_5Cl$ (the 1999-cm^{-1} peak of $Mn(CO)_5Cl$ is obscured by the starting material).

conclude that (η^3-$C_6H_5CH_2$)$Mn(CO)_4$ is fluxional at 200 K and the two structures below are rapidly interconverting.[30]

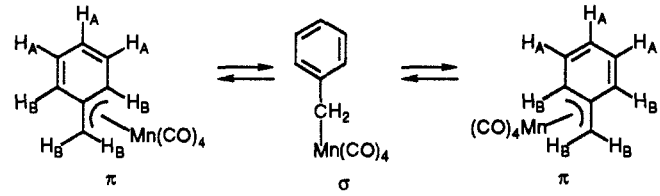

This fluxionality simplifies the ^1H NMR spectrum from that expected if the (η^3-$C_6H_5CH_2$)$Mn(CO)_4$ was stereorigid. This fluxionality is not unexpected as the π–σ–π allyl interconversion should be facile due to the aromatic stabilization of the phenyl ring in the 16e (η^1-$C_6H_5CH_2$)$Mn(CO)_4$. The rapid π–σ–π interconversion is in accord with the observation that reaction of (η^3-$C_6H_5CH_2$)$Mn(CO)_4$ with L = CO or PPh_3 occurs at 200 K (vide infra) to give *cis*-(η^1-$C_6H_5CH_2$)$Mn(CO)_4PPh_3$ (eq 13). Warmup of an NMR sample containing (η^3-$C_6H_5CH_2$)$Mn(CO)_4$ to 295 K results in regeneration of the NMR resonances for (η^1-$C_6H_5CH_2$)$Mn(CO)_5$ at the expense of those for the η^3 species, consistent with results from IR. Likewise, warming the η^3 species results in a disappearance of the 390-nm absorbance and return to the original optical spectrum. Generation of (η^3-$C_6H_5CH_2$)$Mn(CO)_4$ at either 200 or 95 K in MCH in an IR cell shows that the absorbance at 390 nm accompanies the growth of the IR bands assigned to (η^3-$C_6H_5CH_2$)$Mn(CO)_4$.

At 200 K, (η^3-$C_6H_5CH_2$)$Mn(CO)_4$ has a half-life for regeneration of (η^1-$C_6H_5CH_2$)$Mn(CO)_5$ of ~2 h. If the alkane contains 0.1 M PPh_3, irradiation results in the initial formation of only (η^3-$C_6H_5CH_2$)$Mn(CO)_4$. The reaction of (η^3-$C_6H_5CH_2$)$Mn(CO)_4$ and PPh_3 yielding *cis*-(η^1-$C_6H_5CH_2$)$Mn(CO)_4PPh_3$ can be monitored by IR spectroscopy and is complete in ~60 min at 200 K. No (η^1-$C_6H_5CH_2$)$Mn(CO)_5$ is re-formed when the alkane contains 0.1 M PPh_3. This result and the NMR data on the fluxionality of (η^3-$C_6H_5CH_2$)$Mn(CO)_4$ are consistent with the conclusion that the formation of *cis*-(η^1-$C_6H_5CH_2$)$Mn(CO)_4PPh_3$ arises from trapping of the intermediate (η^1-$C_6H_5CH_2$)$Mn(CO)_4$, which is in rapid equilibrium with (η^3-$C_6H_5CH_2$)$Mn(CO)_4$ (eq 13). That is, the bimolecular rate for PPh_3 trapping of (η^1-$C_6H_5CH_2$)$Mn(CO)_4$ is small relative to the rate of intramolecular trapping to give (η^3-$C_6H_5CH_2$)$Mn(CO)_4$, but excess PPh_3 irreversibly traps (η^1-$C_6H_5CH_2$)$Mn(CO)_4$, leading to the eventual

(27) Silverstien, R. M.; Bassler, G. C.; Morrill, T. C. *Spectroscopic Identification of Organic Compounds* 4th ed.; Wiley: New York, 1981; p 230.
(28) (a) Druz, N. N.; Klepikova, V. I.; Labach, M. I.; Kormer, V. A. *J. Organomet. Chem.* **1978**, *162*, 343. (b) Wilkinson, G., Stone, F. G. A., Abel, E. W., Eds. *Comprehensive Organometallic Chemistry*; Pergamon: New York, 1982; Vol. 4, p 29.
(29) Brookhart, M.; Buck, R. C.; Danielson, E. *J. Am. Chem. Soc.* **1989**, *111*, 567, and references therein.
(30) Vrieze, K. In *Dynamic Nuclear Magnetic Resonance Spectroscopy*; Jackman, L. M., Cotton, F. A., Eds.; Academic: New York, 1975; p 441.

Scheme I. Summary of Photochemistry of $(\eta^1\text{-}C_6H_5CH_2)Mn(CO)_5$[a]

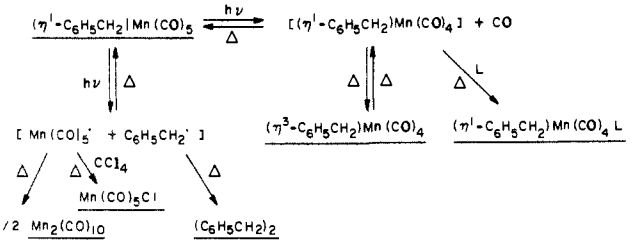

[a] Underlined species have been observed.

net formation of *cis*-$(\eta^1\text{-}C_6H_5CH_2)Mn(CO)_4PPh_3$.

Room-Temperature Photochemistry of $(\eta^1\text{-}C_6H_5CH_2)Mn(CO)_5$. Irradiation (313 nm) of 10^{-3} M $(\eta^1\text{-}C_6H_5CH_2)Mn(CO)_5$ in deoxygenated alkane solution at 295 K leads to rapid formation of $(\eta^3\text{-}C_6H_5CH_2)Mn(CO)_4$ and $Mn_2(CO)_{10}$ in an initial 8:1 ratio (at ~1% consumption of $(\eta^1\text{-}C_6H_5CH_2)Mn(CO)_5$). These two products account for >95% of the $(\eta^1\text{-}C_6H_5CH_2)Mn(CO)_5$ consumed. HPLC analysis of the product mixture following irradiation in MCH shows bibenzyl as the major organic product (~80%). If the alkane solution contains 0.1 M CCl_4, $Mn(CO)_5Cl$ is formed at the expense of $Mn_2(CO)_{10}$, but the yield of the η^3 species and mass balance are unaffected. $(\eta^3\text{-}C_6H_5CH_2)Mn(CO)_4$ is very labile at 295 K and regenerates $(\eta^1\text{-}C_6H_5CH_2)Mn(CO)_5$ with a bimolecular rate constant of 1×10^4 L mol^{-1} s^{-1}; CO added to the alkane solution suppresses the formation of $(\eta^3\text{-}C_6H_5CH_2)Mn(CO)_4$. Prolonged photolysis of $(\eta^1\text{-}C_6H_5CH_2)Mn(CO)_5$ at 295 K leads to a buildup of $Mn_2(CO)_{10}$ (or $Mn(CO)_5Cl$ if the solution contains CCl_4) as the Mn-containing product, since $(\eta^3\text{-}C_6H_5CH_2)Mn(CO)_4$ back-reacts with CO to regenerate the photosensitive $(\eta^1\text{-}C_6H_5CH_2)Mn(CO)_5$. Irradiation (366 nm) of $(\eta^1\text{-}C_6H_5CH_2)Mn(CO)_5$ in alkane solution in the presence of 0.1 M PPh_3 yields mainly *cis*-$(\eta^1\text{-}C_6H_5CH_2)Mn(CO)_4PPh_3$, with a small yield of (<10%) $Mn_2(CO)_8(PPh_3)_2$ via the $Mn(CO)_5$ radicals.[1]

The quantum yield (±10%) was measured for the 295 K photoreaction of $(\eta^1\text{-}C_6H_5CH_2)Mn(CO)_5$ at 366 nm in alkane containing both 0.1 M CCl_4 and 0.1 M PPh_3. The disappearance quantum yield of $(\eta^1\text{-}C_6H_5CH_2)Mn(CO)_5$ is 0.81, while the CO-loss quantum yield, measured by the appearance of $(\eta^1\text{-}C_6H_5CH_2)Mn(CO)_4PPh_3$, is 0.69. The Mn–R bond homolysis quantum yield, measured by the appearance of $Mn(CO)_5Cl$, is 0.08.

Discussion

Consider what we have and have not seen in the two $RMn(CO)_5$ systems studied. Schemes I and II summarize the photochemical processes and the follow-up thermal and photochemical processes for R = $\eta^1\text{-}C_6H_5CH_2$ and $\eta^1\text{-}C_5Cl_5$, respectively. In neither case have we spectroscopically detected any of the primary 16- or 17e Mn species. However, in both cases the η^3-species have been well characterized spectroscopically at low temperature ≤200 K. The $(\eta^3\text{-}C_6H_5CH_2)Mn(CO)_4$ is relatively inert thermally and photochemically with respect to CO loss in comparison to $(\eta^3\text{-}C_5Cl_5)Mn(CO)_4$. The latter species is both thermally and photochemically labile with respect to CO loss, whereas $(\eta^3\text{-}C_6H_5CH_2)Mn(CO)_4$ can be generated essentially quantitatively in rigid media at 95 K with no detectable secondary CO-loss chemistry. The 16e species from photochemical CO loss from $(\eta^5\text{-}C_5Cl_5)Mn(CO)_3$ has been detected and characterized previously.[31]

The results obtained for $RMn(CO)_5$ (R = $\eta^1\text{-}C_5Cl_5$, $\eta^1\text{-}C_6H_5CH_2$) support our main conclusion: Photoexcitation yields *both* CO loss (eq 1) and Mn–R cleavage (eq 2). These two photoprocesses occur at all wavelengths where the molecules absorb, but the importance of CO loss is greater at shorter wavelengths, while Mn–R cleavage is relatively insensitive to the excitation wavelength. For both complexes studied the CO-loss products could arise from axial and/or equatorial CO loss. In

Scheme II. Summary of Photochemistry of $(\eta^1\text{-}C_5Cl_5)Mn(CO)_5$[a]

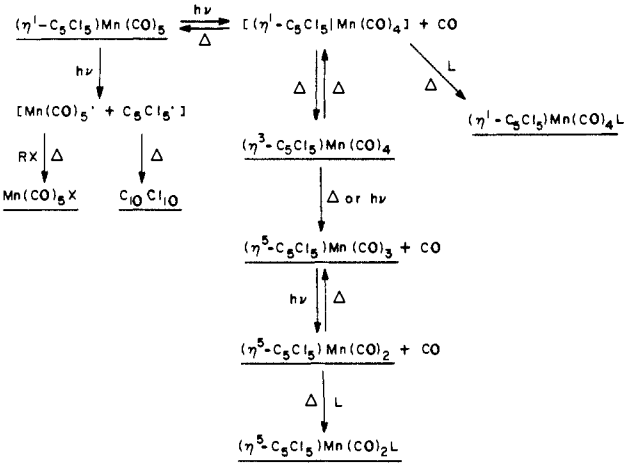

[a] Underlined species have been observed.

the case of R = $\eta^1\text{-}C_5Cl_5$, comparison of photochemistry in the presence and absence of added CO suggests axial CO loss is favored upon long-wavelength excitation, whereas equatorial CO loss occurs as well upon short-wavelength excitation (vide infra). Our quantitative findings are in accord with the qualitative studies of the photochemistry of $RMn(CO)_5$, and it is now evident that the net chemistry is dependent on the excitation wavelength, viscosity of the medium, temperature, and the nature of any additives.

Without added ligating groups, in a low-viscosity alkane reaction medium at 298 K, and under circumstances where photoejected CO cannot escape, the photochemical products from $(\eta^1\text{-}C_6H_5CH_2)Mn(CO)_5$ largely reflect the chemistry of Mn–R cleavage. For $(\eta^1\text{-}C_6H_5CH_2)Mn(CO)_5$ under these conditions the photochemical loss of CO is essentially quantitatively reversible and independent of excitation wavelength. Thus, the Mn–R cleavage process ultimately is the sole source of net products despite the relatively low quantum yield for Mn–R cleavage compared to CO loss. In this regard, the photochemistry of $(\eta^1\text{-}C_6H_5CH_2)Mn(CO)_5$ parallels the photochemistry of $(\eta^5\text{-}C_5R'_5)Fe(CO)_2(\eta^1\text{-}C_6H_5CH_2)$ (R′ = H, CH_3), which also gives radical and CO-loss products.[32] Net products from the CO-loss process for the Fe species are not significant in the absence of added ligands, because the $(\eta^5\text{-}C_5R'_5)Fe(CO)(\eta^3\text{-}C_6H_5CH_2)$ is very labile with respect to back-reaction with CO. Low-temperature photoexcitation of both $(\eta^5\text{-}C_5R'_5)Fe(CO)_2(\eta^1\text{-}C_6H_5CH_2)$[32] and $(\eta^1\text{-}C_6H_5CH_2)Mn(CO)_5$ efficiently yields only an $\eta^3\text{-}C_6H_5CH_2$ species following prompt CO loss. The Mn–$CH_2C_6H_5$ or Fe–$CH_2C_6H_5$ cleavage to give radicals upon photolysis at low temperature is not detectable, presumably because cage escape of the primary radical products is less efficient in the more viscous (or rigid) low-temperature media. In low-temperature (200 K) but fluid media the η^3 species accumulate, because back-reaction with CO is slow. Thus, the near-UV photoproducts from $(\eta^1\text{-}C_6H_5CH_2)Mn(CO)_5$ or $(\eta^5\text{-}C_5R'_5)Fe(CO)_2(\eta^1\text{-}C_6H_5CH_2)$[32] in an alkane are either CO-loss or radical-derived depending on whether the reaction is carried out at 200 or 295 K, respectively. An important fact, however, is that our studies show that the 295 K radical formation is a *primary* process that occurs at only a fraction (~10%) of the CO-loss process.

The results from $(\eta^1\text{-}C_5Cl_5)Mn(CO)_5$, in terms of assessing the primary photochemical processes, are somewhat easier to interpret than the results from $(\eta^1\text{-}C_6H_5CH_2)Mn(CO)_5$, because the photochemical products in the *absence* of additives are revealing with respect to the nature of the primary photoprocesses. The photoproducts at 295 K in alkanes reflect the nature of the primary photoprocesses, because CO loss to give an $\eta^3\text{-}C_5Cl_5$ intermediate is followed (thermally) by a rapid process to give an inert species, $(\eta^5\text{-}C_5Cl_5)Mn(CO)_3$. Thus, the ring slippage "traps" the CO-loss

(31) Young, K. M.; Wrighton, M. S. *Organometallics* **1989**, *8*, 1063.

(32) Blaha, J. P.; Wrighton, M. S. *J. Am. Chem. Soc.* **1985**, *107*, 2694.

Scheme III. Electronic Structure of $RMn(CO)_5$

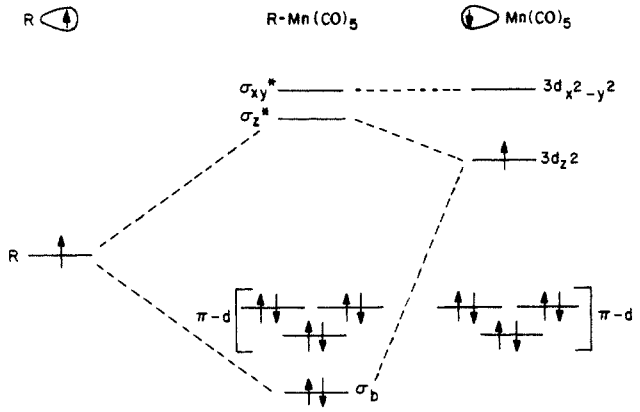

product. It is clear that $(\eta^3\text{-}C_5Cl_5)Mn(CO)_4$ can back-react with CO to give $(\eta^1\text{-}C_5Cl_5)Mn(CO)_5$ in competition with ring slippage to give $(\eta^5\text{-}C_5Cl_5)Mn(CO)_3$. However, such competition is not efficient at low extent conversions of low concentrations, because the CO concentration is small. The radical formation from Mn–R cleavage in $(\eta^1\text{-}C_5Cl_5)Mn(CO)_5$ is revealed by the formation of $Mn(CO)_5Cl$.

The wavelength dependence of the photochemistry of $(\eta^1\text{-}C_5Cl_5)Mn(CO)_5$ shows that CO loss is actually less important than Mn–R cleavage at long wavelengths, while CO loss is dominant at short wavelengths. The effect of added CO on the primary product distribution reveals that there must be two different CO-loss products, one of which is more quenchable by added CO and one of which is less quenchable by added CO. Shorter wavelengths give a CO-loss process that is less quenchable, Table III, than do longer wavelengths. We propose that the less quenchable CO-loss process is one that involves the loss of a CO cis to the $\eta^1\text{-}C_5Cl_5$ group. The more quenchable CO-loss process is proposed to be the loss of the CO trans to the $\eta^1\text{-}C_5Cl_5$. Analogous data have not been obtained for $(\eta^1\text{-}C_6H_5CH_2)Mn(CO)_5$, and the relative importance of axial and equatorial CO loss cannot be evaluated. Scheme III shows an orbital diagram useful in providing a rationale for the wavelength-dependent photochemistry and for the effect of added CO as a function of excitation wavelength for $(\eta^1\text{-}C_5Cl_5)Mn(CO)_5$. Axial CO loss is expected from electronic excited states involving population of the σ^*_z orbital, whereas excited states involving the population of σ^*_{xy} should labilize the equatorial CO's.[1] The added CO is believed to more efficiently intercept the 16e species derived from the loss of the trans CO, because there appears to be more rearrangement required to achieve the ring-slipped $(\eta^3\text{-}C_5Cl_5)Mn(CO)_4$ from this intermediate than when a CO is lost from the cis position.

Comment on the electronic structure of $RMn(CO)_5$ and its photochemical reactivity is appropriate. All of the excited states of $RMn(CO)_5$ involving population of the σ^* levels arising from the Mn $3d_{x^2-y^2}$, $3d_{z^2}$, and ligand σ-orbitals should be labile with respect to dissociative processes. The wavelength-dependent photochemistry allows the conclusion that at least *two* different excited states yield chemistry. Since long-wavelength excitation appears to favor Mn–R cleavage compared to CO loss, and the CO loss that occurs at long wavelength is more quenchable and attributed to loss of the trans CO, we conclude that long-wavelength excitation results in predominantly population of the σ^* level derived from the $3d_{z^2}$ orbital, σ^*_z. The population of this orbital results in a degree of selectivity with respect to labilization of ligands on the z-axis, R, and the trans CO. Population of the σ^* orbital derived from $3d_{x^2-y^2}$, σ^*_{xy}, at higher energy, labilizes the cis CO's. It should be appreciated that the upper excited state likely competitively relaxes to the lower excited state, accounting for significant Mn–R cleavage upon short-wavelength excitation.

The orbital origin of the transitions that terminate in the σ^* orbitals of $RMn(CO)_5$ is possibly the filled π–d set. As in other C_{4v} low-spin d^6 systems the first absorption is then associated with the $e(d_{xz},d_{yz}) \rightarrow a_1(d_{z^2})$ transition.[1,33] However, in the cases of $RMn(CO)_5$ studied, the R group is not a weak field ligand compared to CO, and the splitting of the $a_1(d_{z^2})$ and $b_1(d_{x^2-y^2})$ σ^* levels is not as great as in species like $Mn(CO)_5Cl$ where Cl^- is a much weaker field ligand than CO.[1] Considering the fact that the $RMn(CO)_5$ complexes studied have six strong field ligands, it is somewhat surprising to see such strong wavelength effects in the photochemistry within the framework of ligand field excited states. For this reason it is tempting to invoke a role for the $\sigma_b \rightarrow \sigma^*_z$ transition that would be analogous to the $\sigma_b \rightarrow \sigma^*$ transition in $Mn_2(CO)_{10}$.[34] The $\sigma_b \rightarrow \sigma^*$ excited state in $RMn(CO)_5$ is likely to at least be close in energy to the π–d $\rightarrow \sigma^*_z$ excited states, and the *triplet* $\sigma_b \rightarrow \sigma^*_z$ may be lowest in energy. It is perhaps noteworthy that $Mn_2(CO)_{10}$ shows both CO loss and Mn–Mn cleavage, with CO loss being more efficient at shorter wavelengths.[35] These findings with $Mn_2(CO)_{10}$ parallel what we have now found for $RMn(CO)_5$. Our principal conclusion regarding electronic structure and reactivity is that the photochemical reactions of $RMn(CO)_5$ all are mainly due to the great degree of lability associated with population of the σ^*_z or σ^*_{xy} orbitals. However, the orbital origin of the reactive excited states is uncertain. The optical absorption spectrum of $RMn(CO)_5$ would appear to be consistent with π–d $\rightarrow \sigma^*$ transitions. The absorptions, though, are due to singlet $\rightarrow$ singlet absorption and do not reveal the location of the triplet excited states.

The electronic structure of $(\eta^1\text{-}C_5Cl_5)Mn(CO)_5$ deserves special comment because C_5Cl_6 gives C_5Cl_5 and Cl upon photoexcitation.[36] The point is that C_5Cl_6 absorbs in the same region as $(\eta^1\text{-}C_5Cl_5)Mn(CO)_5$, Figure 1, and we could view the $RMn(CO)_5$ species as C_5Cl_5X where X is the "pseudohalogen" $Mn(CO)_5$. When our system is viewed as C_5Cl_5X, it is reasonable to ask whether photoexcitation results in C–Cl homolysis at the carbon bearing the X = $Mn(CO)_5$ group. We find no evidence for such photochemistry, specifically none at low temperature in a matrix where C_5Cl_6 is photosensitive. The similarity of the wavelength dependence of the photochemistry of $(\eta^1\text{-}C_5Cl_5)Mn(CO)_5$ and $(\eta^1\text{-}C_6H_5CH_2)Mn(CO)_5$ suggests common excited states, and we favor the electronic structural view emphasizing the $RMn(CO)_5$ chromophore, Scheme III. It is important to recognize, however, that there are some important similarities between the bonding of X = $Mn(CO)_5$ and X = Cl in C_5Cl_5X and that there is merit in viewing our system as a derivative of C_5Cl_6 rather than as a $RMn(CO)_5$ species. The photochemical results found justify our view that the $(\eta^1\text{-}C_5Cl_5)Mn(CO)_5$ behaves in a manner similar to other $RMn(CO)_5$ species where the R group has no reactive excited states in the same energy regime.

The final point to be made concerns the thermal lability of the η^3 species formed from the $RMn(CO)_5$ complexes. Both η^3 species react rapidly with 2e-donor ligands presumably via a first step to form a 16e η^1-R complex. The $\eta^3 \rightleftarrows \eta^1$ conversion appears to be fast for both the R = $C_6H_5CH_2$ and C_5Cl_5 cases, and 2e-donor ligands can compete effectively for the open site created by the $\eta^3 \rightarrow \eta^1$ conversion. Interestingly, the $(\eta^3\text{-}C_5Cl_5)Mn(CO)_4$ reacts with sufficiently high concentrations of a 2e-donor ligand completely competitively to form $(\eta^1\text{-}C_5Cl_5)Mn(CO)_4L$, and no ring slippage to form the inert $(\eta^5\text{-}C_5Cl_5)Mn(CO)_3$ is detected. These results suggest that there may be the need to consider $\eta^3 \rightarrow \eta^1$ conversion in situations where $\eta^5 \rightarrow \eta^3$-cyclopentadienyl processes are involved in substitution and oxidative addition processes of η^5-cyclopentadienyl complexes. It is known that some 17e $\eta^5\text{-}C_5H_5$[37] or η^5-indenyl[38] complexes add CO with great facility to

(33) (a) Vogler, A. In *Concepts of Inorganic Photochemistry*; Adamson, A. W., Fleischauer, P. D., Eds.; Robert E. Krieger: Malabar, FL, 1984. (b) Wrighton, M. S.; Morse, D. L.; Gray, H. B.; Ottesen, D. K. *J. Am. Chem. Soc.* **1976**, *98*, 1111.

(34) Levenson, R. A.; Gray, H. B.; Ceasar, G. P. *J. Am. Chem. Soc.* **1970**, *92*, 3653.

(35) Seder, T. A.; Church, S. P.; Weitz, E. *J. Am. Chem. Soc.* **1986**, *108*, 7518. Hepp, A. F.; Wrighton, M. S. *J. Am. Chem. Soc.* **1983**, *105*, 5935. Meyer, T. J.; Caspar, J. V. *Chem. Rev.* **1985**, *85*, 187.

(36) (a) Graf, F.; Gunthard, Hs. H. *Chem. Phys. Lett.* **1970**, *7*, 25. (b) Bachmann, P.; Graf, F.; Gunthard, Hs. H. *Chem. Phys.* **1975**, *9*, 41.

(37) van Raaij, E. U.; Brintzinger, H.-H. *J. Organomet. Chem.* **1988**, *356*, 315.

give η^3 species, but further slippage to η^1 species has not been reported. However, it is important to note that in the absence of 2e-donor ligands the rate of thermal conversion of $(\eta^3$-$C_5Cl_5)Mn(CO)_4$ to $(\eta^5$-$C_5Cl_5)Mn(CO)_3$ at 220 K is 10^4 times slower than the extrapolated rate for the conversion of $(\eta^5$-$C_5H_5)(\eta^3$-$C_5H_5)Fe(CO)$ to $(\eta^5$-$C_5H_5)_2Fe$.[19] This decrease in the thermal ring slippage rate is presumably due to the electron-withdrawing effect of the Cl substituents on the cyclopentadienyl ring, which slows the coordination from that found in the C_5H_5 case. The importance of $\eta^3 \rightarrow \eta^1$-$C_5H_5$ conversion versus the $\eta^3 \rightarrow \eta^5$-$C_5H_5$ process requires experimental investigation.

Acknowledgment. We thank the National Science Foundation for support of this research. In addition, K.M.Y. is grateful to the Natural Sciences and Engineering Research Council of Canada for support as a graduate fellow, 1985-1989.

Registry No. $(\eta^1$-$C_5Cl_5)Mn(CO)_5$, 53158-67-1; $(\eta^3$-$C_5Cl_5)Mn(CO)_4$, 123001-82-1; $(\eta^5$-$C_5Cl_5)Mn(CO)_3$, 56282-21-4; *cis*-$(\eta^1$-$C_5Cl_5)Mn(CO)_4PPh_3$, 122967-78-6; $Mn(CO)_5Cl$, 14100-30-2; $Mn(CO)_5Br$, 14516-54-2; $Mn(CO)_5I$, 14879-42-6; $Mn_2(CO)_{10}$, 10170-69-1; $[Mn(CO)_4Cl]_2$, 18535-43-8; $(\eta^1$-$C_6H_5CH_2)Mn(CO)_5$, 14049-86-6; $(\eta^3$-$C_6H_5CH_2)Mn(CO)_4$, 122967-79-7; *cis*-$(\eta^1$-$C_6H_5CH_2)Mn(CO_4)PPh_3$, 54834-89-8; $C_{10}Cl_{10}$, 2227-17-0; $C_{10}Cl_8$, 6298-65-3; C_5Cl_6, 77-47-4; $(C_6H_5CH_2)_2$, 103-29-7; $(\eta^5$-$C_5Cl_5)Mn(CO)_2$, 119272-39-8; $[(\eta^5$-$C_5H_5)Fe(CO)_2]_2$, 12154-95-9; $(\eta^5$-$C_5H_5)Fe(CO)_2Cl$, 12107-04-9.

(38) Kowaleski, R. M.; Rheingold, A. L.; Trogler, W. C.; Basolo, F. *J. Am. Chem. Soc.* **1986**, *108*, 2460.
(39) Pope, K. R.; Wrighton, M. S. *J. Am. Chem. Soc.* **1987**, *109*, 4545.

Synthesis and Characterization of a Paramagnetic Osmium-Ruthenium Double Bond

James P. Collman* and James M. Garner

Contribution from the Chemistry Department, Stanford University, Stanford, California 94305.
Received January 6, 1989

Abstract: Using a cofacial biphenylene-bridged bis(porphyrin) (DPB, 1,8-bis[5-(2,8,13,17-tetraethyl-3,7,12,18-tetramethyl)porphyrin]biphenylene), a general synthetic method for the preparation of heterodinuclear complexes with 3d, 4d, and 5d transition metals is described. For $(Os^{II})(Ru^{II})$DPB, and DPB ligand provides a high local concentration of the mixed-metal pair, thereby controlling the stoichiometry of the metal-metal interaction and facilitating the formation of an intramolecular, paramagnetic, osmium-ruthenium double bond. The magnetic and spectroscopic properties are found to be similar to those of the analogous homodinuclear ruthenium and osmium DPB compounds.

Heteronuclear metal-metal multiple bonds in complexes with $L_4MM'L_4$ structures remain a curiosity within this subfield of inorganic chemistry. The molecular orbital diagram,[1] which correctly predicts many of the physical properties of homonuclear dimers with this structure, can be used to predict that numerous heteronuclear combinations of transition metal should also form the same types of metal-metal multiple bonds (Figure 1).[2] However, few of these compounds have yet to be prepared and characterized.[3] The problem is likely not the intrinsic thermodynamic instability of such heteronuclear metal-metal bonds relative to their homonuclear counterparts but, rather, the lack of convergent synthetic methods for their preparation and isolation. Problems associated with indirect methods for the preparation of heteronuclear metal-metal bonds can be illustrated by the reaction in eq 1. Vacuum pyrolysis of an intimate mixture of

$$Ru(OEP)(Py)_2 + Os(OEP)(Py)_2 \rightarrow [Ru(OEP)]_2 + [(OEP)RuOs(OEP)] + [Os(OEP)]_2 \quad (1)$$

mononuclear Ru and Os porphyrin bis(pyridine) complexes yields a nonstoichiometric mixture of three products as determined by ^1H NMR.[4] Two of these products are identified as the homonuclear Ru and Os porphyrin dimers, and the new complex is postulated as the heteronuclear dimer containing a paramagnetic Os=Ru bond. Attempts to isolate the heteronuclear dimer in order to study its magnetic, spectroscopic, and chemical properties are difficult due to the similarity in physical properties (solubility, instability on chromatographic supports, etc.) to the mononuclear dimers. Hence, difficulties in controlling stoichiometry and isolating the heteronuclear product from other reaction products frustrate the synthesis of these interesting compounds.

Our approach to solving this problem originates from another research project within our group concerning the development of molecular catalysts for the reduction of dioxygen via the four-electron pathway. Most of the successful catalysts for this reaction utilize a cofacial bis(porphyrin) ligand, which allows two 3d metals to be held in close proximity such that both can act cooperatively in the reduction of an axially bound dioxygen molecule.[5] For 4d and 5d transition metals, it seemed likely that such ligands allow a sufficiently close approach of the two metals that strong metal-metal bonding interactions would occur in the absence of axial ligands. We have since demonstrated this with the synthesis and characterization of the homonuclear compounds, $(Ru^{II})_2$DPB and $(Mo^{II})_2$DPB (DPB represents a biphenylene-bridged cofacial bis(porphyrin); Figure 2). The presence of intramolecular metal-metal bonds in these compounds is based upon magnetic susceptibility, ^1H NMR, and UV-visible similarities to the analogous OEP dimers.[6]

(1) Cotton, F. A.; Curtis, N. F.; Harris, C. B.; Johnson, B. F. G.; Lippard, S. J.; Mague, J. T. *Robinson*, W. R.; Wood, J. S. *Science* **1964**, *145*, 1305.
(2) As pointed out to us by Prof. Cotton, the spin states of some of the heteronuclear compounds tabulated in this figure may differ from these predicted values. For example, he and others have shown that the δ^* and π^* metal-metal orbitals for the mixed-valence compound, $Ru_2(O_2CC_3H_7)_4Cl$, are close in energy, leading to a quartet instead of a doublet spin state. However, all of the present data for the homonuclear porphyrin dimers is consistent with metal-metal orbitals, which are well separated in energy [i.e., $[Ru(OEP)]_2^+(BF_4^-)$ is low spin, $\mu_{eff} = 1.8 \pm 0.3\ \mu_B$). We must therefore wait for the compounds to be prepared to see whether the spin-state predictions hold true.
(3) Morris, R. H. *Polyhedron* **1987**, *6*, 793. This paper gives a review of quadruply bonded, chromium triad heterodinuclear complexes.
(4) Barnes, C. E. Ph.D. Thesis, Stanford University, 1982. Woo, L. K. Ph.D Thesis, Stanford University, 1984.
(5) (a) Collman, J. P.; Hendricks, N. H.; Leidner, C. R.; Ngameni, E.; L'Her, M. *Inorg. Chem.* **1988**, *27*, 387, and references therein. (b) Ni, C.; Abdalmuhdi, I.; Chang, C. K.; Anson, F. C. *J. Chem.* **1987**, *91*, 1158.
(6) Collman, J. P.; Kim, K.; Garner, J. M. *J. Chem. Soc., Chem. Commun.* **1986**, 1711.

0002-7863/90/1512-166$02.50/0